

The application of green $\text{YF}_3:\text{Er}^{3+}, \text{Yb}^{3+}$ and red $\text{MgSr}_3\text{Si}_2\text{O}_8:\text{Eu}^{2+}, \text{Mn}^{2+}$ layers to remote phosphor LED

My Hanh Nguyen Thi¹, Nguyen Thi Phuong Loan², Nguyen Doan Quoc Anh³

¹Faculty of Mechanical Engineering, Industrial University of Ho Chi Minh City, Vietnam

²Faculty of Fundamental 2, Posts and Telecommunications Institute of Technology, Vietnam

³Power System Optimization Research Group, Faculty of Electrical and Electronics Engineering, Ton Duc Thang University, Vietnam

Article Info

Article history:

Received Aug 7, 2019

Revised Jun 30, 2020

Accepted Jul 9, 2020

Keywords:

Color rendering index

Lumen output

$\text{MgSr}_3\text{Si}_2\text{O}_8:\text{Eu}^{2+}, \text{Mn}^{2+}$

WLEDs

$\text{YF}_3:\text{Er}^{3+}, \text{Yb}^{3+}$

ABSTRACT

White light-emitting diodes (WLEDs) with quantum dots (QDs) and phosphor have pulled in huge consideration because of their incredible shading rendering capacity. In the bundling procedure, a QDs film and a phosphor silicone layer will in general be isolated for lessening the reabsorption misfortunes and keeping the QDs surface molecules in a good condition. This examination explored the bundling succession of QDs and phosphor layers to the optical and warm exhibitions of WLEDs. The emitted optical power and PL spectra were estimated and dissected, while an infrared warm imager was utilized to reenact and approve tentatively the temperature fields. The results reveal that at 60 mA, WLEDs with green QDs-on-phosphor type accomplished lumen output (LO) of 1578 lm, with shading rendering record (CRI) of $R_a = 60$, while the red QDs-on-phosphor type WLEDs exhibited lower LO of 1000 lm, with $R_a = 82$. In addition, the QDs-on-phosphor type WLEDs generated less warmth than the other, and as a result, the most noteworthy temperature in this packaged type was lower than the other. Additionally, its temperature contrast can arrive at 12.3°C . Along these lines, regarding bundling arrangement, the QDs-on-phosphor type is an ideal bundling design to better the optical productivity and shading rendering capacity, as well as lower gadget temperature.

This is an open access article under the [CC BY-SA](https://creativecommons.org/licenses/by-sa/4.0/) license.



Corresponding Author:

Nguyen Doan Quoc Anh,
Power System Optimization Research Group,
Faculty of Electrical and Electronics Engineering,
Ton Duc Thang University,
Ho Chi Minh City, Vietnam.
Email: nguyendoanquocanh@tdtu.edu.vn

1. INTRODUCTION

Phosphor converted-light-emitting diodes (pc-LEDs) have gained its popularity in the lighting market and been considered as a great alternative light source to the conventional one. Moreover, with their outstanding features, including high radiant productivity lighting efficacy (LE), low energy consumption, and long lifespan, they also become favorable in strong state lighting (SSL) and level board show applications [1-3]. The most regular pc-LEDs are acknowledged by putting yellow phosphor $\text{Y}_3\text{Al}_5\text{O}_{12}:\text{Ce}^{3+}$ (YAG: Ce^{3+}) on the surface of blue LED chips. Some portion of blue lights from the LED chips are consumed by the phosphor and changed into yellow light, and then the white light is generated as a result of the combination between the blue light and yellow light. This sort of pc-LEDs can arrive at high LE, while their shading rendering record (CRI) is fairly poor because of the red phantom inadequacy [4]. Numerous endeavors have been proposed and carried out to

improve the shading rendering capacities for pc-LEDs, for example, the expansion of high effectiveness red emissive phosphors [5-8]. Be that as it may, they are unequipped for keeping up high LE in light of the fact that their wide red discharge in part is not in the delicate locale of human eyes [8, 9]. As of late, semiconductor quantum dabs (QDs) have pulled in various considerations in SSL applications by uprightness of their unique optical properties, for example, restricted discharge spectra, tunable band-hole, and high quantum efficiency [10-13]. Researches have demonstrated hypothetically and tentatively that including QDs in pc-LED packages can achieve a significant improvement in color rendering index (CRI) and shading extent and QDs' tight emanation takes into consideration the capability of better luminous efficacy [14-16]. The noteworthy bundling procedures of applying QDs to pc-LEDs includes the two approaches: 1) The blended structure in which the LED chips are coated with the mixture of QDs and phosphor-silicone gel [17, 18]; 2) a QDs layer and a phosphor film are separately placed on the LED chips, which is called the remote structure [19, 20]. For the blended structure, the QDs that are put into the reflection cup is placed on the LED chips. In this manner, the QDs experience the ill effects of a high optical power thickness. Meanwhile, the remote phosphor design shows that the QDs film is separated from the chip, and consequently experiencing a lower optical power thickness. Moreover, it is possible to discharge the substance incongruence between the surface of QDs' ligands and the phosphor-silicone gel by making a change to the polymeric condition of QDs film [21-23]. In this manner, the remote bundling structure is generally used for creating WLEDs with both QDs and phosphor.

2. PREPARATION AND SIMULATION

In type I, as illustrated in Figure 1 (a), the green QDs layer is located above the yellow phosphor layer while in type II as shown in Figure 1 (b) on the phosphor layer is the red QDs film. The bundling succession can influence the light output productivity, and thus changing the temperature dispersion, and at last impacts the long-haul soundness. Albeit numerous sorts of writing have talked about the impact of bundling design on the performance of QDs-WLEDs, there is no deliberate investigation about the optical vitality move between the QDs and the phosphor layers. Then, Woo and his partners right off the bat looked at two structures QDs-on-phosphor and phosphor-on-QDs with their examination in the PL rot of QDs and phosphor. Their outcomes give huge direction to QDs-WLEDs plan. In any case, they did not discover the loss of the optical vitality of QDs and phosphor in these two types of layered structures, and moreover the variety of QDs content on the exhibition variety has not been considered. Along these lines, in this work, we conducted quantitative researches on the presentation contrasts between the two sorts of WLEDs by exactly restricting the optical vitality loss of QDs and phosphor. The red CdSe/ZnS QDs were joined, and WLED packages were manufactured dependently on YAG:Ce³⁺ phosphor layer and a progression of QDs layer. An incorporating circle framework was used to estimate and break down the yield optical power and PL spectra, while a process of brushing optical estimation with warm reenactment was applied to recreate the temperature fields which were finally approved with the use of infrared warm imager. It was confirmed that among the bundling structures, the QDs-on-phosphor type is the most appropriate design to accomplish higher optical efficiency and shading rendering capacity, along with lower temperature for the devices.

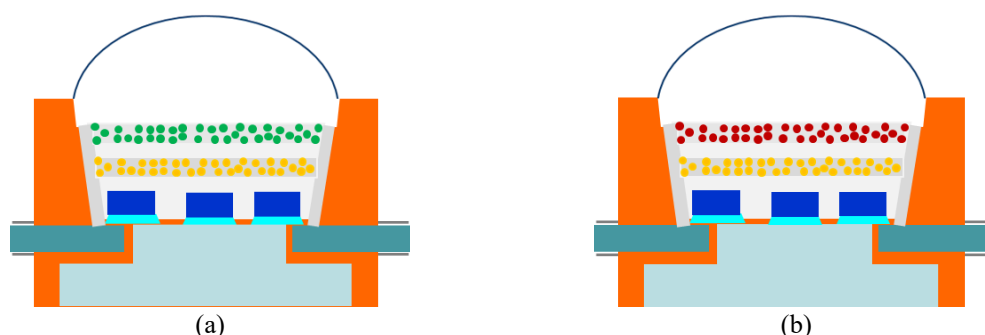


Figure 1. Schematic showing two remote type WLEDs with different packaging sequences; (a) green QDs-on-phosphor type, (b) red QDs-on-phosphor type

3. RESULTS AND DISCUSSION

Figure 2 showed the conflicting alteration among the green phosphor fixation YF₃:Er³⁺,Yb³⁺, red phosphor focus MgSr₃Si₂O₈:Eu²⁺,Mn²⁺, and yellow phosphor focus YAG:Ce³⁺. This adjustment has two implications: the principal importance is to keep up the normal of CCTs and the subsequent one is that it

The application of green YF₃:Er³⁺,Yb³⁺ and red MgSr₃Si₂O₈:Eu²⁺,Mn²⁺... (My Hanh Nguyen Thi)

influences to the dispersing and engrossing procedure of two phosphor layers in WLEDs, which certainly influences to the shading quality and radiant transition discharge of WLEDs. Henceforth, the decision of $\text{YF}_3:\text{Er}^{3+}, \text{Yb}^{3+}$ and $\text{MgSr}_3\text{Si}_2\text{O}_8:\text{Eu}^{2+}, \text{Mn}^{2+}$ focus decides shading nature of WLEDs. At the point when the $\text{YF}_3:\text{Er}^{3+}, \text{Yb}^{3+}$, and $\text{MgSr}_3\text{Si}_2\text{O}_8:\text{Eu}^{2+}, \text{Mn}^{2+}$ fixation individually increment from 2%-20% wt., YAG: Ce^{3+} focus diminishes to keep up the normal of CCTs. It is anything but difficult to understand the impact of red phosphor fixation $\text{MgSr}_3\text{Si}_2\text{O}_8:\text{Eu}^{2+}, \text{Mn}^{2+}$ on outflow range of WLEDs as Figure 3.

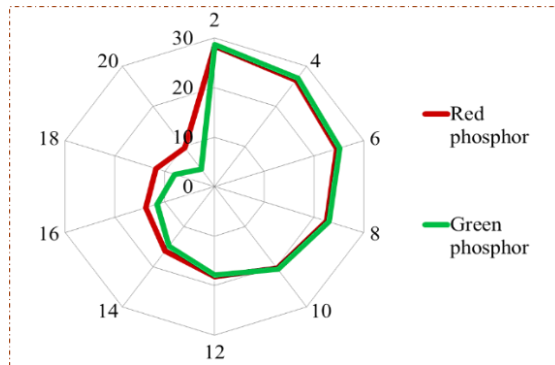


Figure 2. The change of phosphor concentration of the remote WLEDs for keeping the average CCT

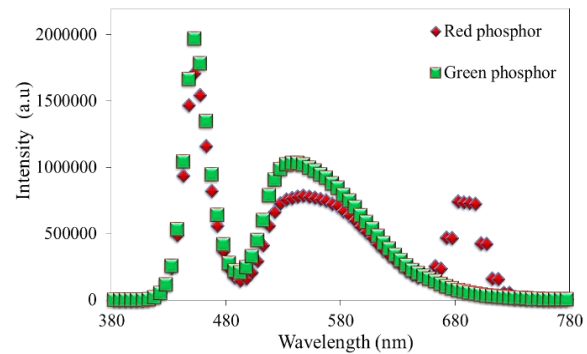


Figure 3. Emission spectra of dual-layer phosphor configurations

The decision relies upon the prerequisite of maker. WLEDs require high shading quality, so it is conceivable to diminish a little measure of glowing transition. The force inclination at two light range ranges from 420-480 nm to 500-640 nm will in general increment with $\text{YF}_3:\text{Er}^{3+}, \text{Yb}^{3+}$ focus. The expansion of range transmitted in this range demonstrates for the expansion of radiant transition emanation. Furthermore, blue-light dispersing in WLED builds which implies that the dissipating in phosphor layer and WLEDs expands prompts a few focal points for the connected shading. This is an astounding outcome in applying $\text{YF}_3:\text{Er}^{3+}, \text{Yb}^{3+}$. It is evident to understand that the inclination of red range ranges from 648 to 738 nm increments with $\text{MgSr}_3\text{Si}_2\text{O}_8:\text{Eu}^{2+}, \text{Mn}^{2+}$ fixation. Be that as it may, there is no critical significance if coming up short on the expansion of two range ranges left: 420-480 nm and 500-640 nm. The expansion of two ranges 420-480 nm builds blue-light dispersing. The higher temperature communicates the higher range produced, and the outcome is the higher shading quality and brilliant motion. This is a fundamental outcome applying $\text{MgSr}_3\text{Si}_2\text{O}_8:\text{Eu}^{2+}, \text{Mn}^{2+}$. Particularly, the guideline of shading nature of WLEDs having high temperature is a test. This exploration asserts that $\text{MgSr}_3\text{Si}_2\text{O}_8:\text{Eu}^{2+}, \text{Mn}^{2+}$ can lift shading nature of WLEDs paying little respect to the shading temperature.

Color rendering index truthfully accesses the color of the object when the light of led illuminates too. The measure of green-light increment overwhelmingly which makes the shading unbalance among three noteworthy hues: blue, yellow, and green. This likewise influences the shading quality and prompts a decline of shading honesty of WLEDs. The outcome in Figure 4 showed the slight lessening of CRI when layer remote phosphor $\text{YF}_3:\text{Er}^{3+}, \text{Yb}^{3+}$ exists. Be that as it may, it is worthy since CRI is only a component of CQS. Looking at among CRI and CQS, the list of CQS is increasingly significant and hard to accomplish. In Figure 5, CQS is unchangeable when the $\text{YF}_3:\text{Er}^{3+}, \text{Yb}^{3+}$ concentration under 8%. In this way, 8% $\text{YF}_3:\text{Er}^{3+}, \text{Yb}^{3+}$ can be picked to apply in the wake of thinking about the glowing transition outflow. The model of the asymmetrical spectrum power distribution (SPD) of monochrome LED is carried out with Gaussian function [24, 25]:

$$P_\lambda = P_{opt} \frac{1}{\sigma\sqrt{2\pi}} \exp \left[-0.5 * \frac{(\lambda - \lambda_{peak})^2}{\sigma^2} \right] \quad (1)$$

in which σ is a parameter depending on the peak wavelength λ_{peak} , and $FWHM \Delta\lambda$ can be expressed as

$$\sigma = \frac{\lambda_{peak}^2 \Delta E}{2hc\sqrt{2\ln 2}} = \frac{\lambda_{peak}^2 \left(\frac{hc}{\lambda_1} - \frac{hc}{\lambda_2} \right)}{2hc\sqrt{2\ln 2}} = \frac{\lambda_{peak}^2 \left(\frac{hc\Delta\lambda}{\lambda_1\lambda_2} \right)}{2hc\sqrt{2\ln 2}} \quad (2)$$

$$P_\lambda = P_{opt,b} \frac{1}{\sigma_b\sqrt{2\pi}} \exp \left[-0.5 * \frac{(\lambda - \lambda_{peak,b})^2}{\sigma_b^2} \right]$$

$$\begin{aligned}
& +P_{opt_g} \frac{1}{\sigma_g \sqrt{2\pi}} \exp \left[-0.5 * \frac{(\lambda - \lambda_{peak_g})^2}{\sigma_g^2} \right] \\
& +P_{opt_y} \frac{1}{\sigma_y \sqrt{2\pi}} \exp \left[-0.5 * \frac{(\lambda - \lambda_{peak_y})^2}{\sigma_y^2} \right]
\end{aligned} \quad (3)$$

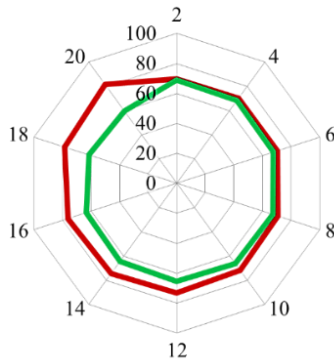


Figure 4. The color rendering index as a function of the concentration of $YF_3:Er^{3+}, Yb^{3+}$ and $MgSr_3Si_2O_8:Eu^{2+}, Mn^{2+}$ phosphors

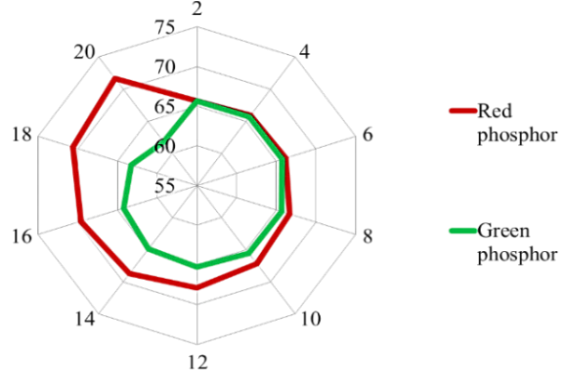


Figure 5. The color quality scale as a function of the concentration of $YF_3:Er^{3+}, Yb^{3+}$ and $MgSr_3Si_2O_8:Eu^{2+}, Mn^{2+}$ phosphors

It is possible to hypothetically consider the SPD of a white LED using yellow YAG phosphor and blue LED chip as a combination between the spectra of the blue and yellow lights. However, in fact, the applied yellow phosphor can emit lights in both yellow and green spectra. In the case where a blue and a yellow range are chosen, a green range can be used to present the contrast between the essentially estimated SPD and twofold shading (blue and yellow shading) range model. Thus, in this practical circumstance, a green range is possibly added to the twofold range model, resulting in the accompanying investigative triple-spectrum (B-G-Y) model which is expressed by (3) and then replaced with (4).

$$\begin{aligned}
P_\lambda &= \eta_b P_{opt_total} \frac{1}{\sigma_b \sqrt{2\pi}} \exp \left[-0.5 * \frac{(\lambda - \lambda_{peak_b})^2}{\sigma_b^2} \right] \\
&+ \eta_g P_{opt_total} \frac{1}{\sigma_g \sqrt{2\pi}} \exp \left[-0.5 * \frac{(\lambda - \lambda_{peak_g})^2}{\sigma_g^2} \right] \\
&+ \eta_y P_{opt_total} \frac{1}{\sigma_y \sqrt{2\pi}} \exp \left[-0.5 * \frac{(\lambda - \lambda_{peak_y})^2}{\sigma_y^2} \right]
\end{aligned} \quad (4)$$

in which:

- P_λ is spectrum power distribution (SPD) (mW/nm).
- h is planck's constant (J.s).
- c is speed of light ($m\ s^{-1}$).
- λ is wavelength (nm).
- P_{opt} is optical power (W).
- λ_{peak} is peak wavelength (nm).
- $\Delta\lambda$ indicates full-width at half-maximum (FWHM) (nm).
- η presents the ratio of specific spectra to white spectrum, dimensionless.
- P_{opt_b} , P_{opt_g} , P_{opt_y} , and P_{opt_total} express the optical power (W) for the blue, green, yellow, and white spectra, respectively.
- λ_{peak_b} , λ_{peak_g} , and λ_{peak_y} are peak wavelengths (nm) for the blue, green, and yellow spectra, respectively.
- η_b , η_g , and η_y show the ratios of blue-green-yellow (B-G-Y) spectra to white spectrum, respectively, dimensionless.
- λ_1 and λ_2 indicate wavelengths at half of the peak intensity.

Hence, the model of SPD for the WLED with phosphor-coated design can be demonstrated as a tricolor spectrum, and this is viewed as an extended Gaussian model. Figure 6 demonstrates that radiant

motion expanded considerably when $\text{YF}_3:\text{Er}^{3+}, \text{Yb}^{3+}$ rise in the range of 2-20% wt. Be that as it may, the grouping of phosphor $\text{MgSr}_3\text{Si}_2\text{O}_8:\text{Eu}^{2+}, \text{Mn}^{2+}$ impacts the brilliant transition of dual-layer remote phosphor configuration. Obviously, as per Lambert-Beer law, the decreased factor μ_{ext} is proportional to the grouping of $\text{MgSr}_3\text{Si}_2\text{O}_8:\text{Eu}^{2+}, \text{Mn}^{2+}$, but contrarily relative to the light transmission vitality. Along these lines, if the thickness of two phosphor layers in WLEDs are fixed, the radiant transition radiated may diminish when the grouping of $\text{MgSr}_3\text{Si}_2\text{O}_8:\text{Eu}^{2+}, \text{Mn}^{2+}$ increments. At the point when fixation of $\text{MgSr}_3\text{Si}_2\text{O}_8:\text{Eu}^{2+}, \text{Mn}^{2+}$ at 20% wt optics diminished altogether. Be that as it may, this decrease is flawlessly adequate, when considering the upsides of the red phosphor class $\text{MgSr}_3\text{Si}_2\text{O}_8:\text{Eu}^{2+}, \text{Mn}^{2+}$ which are increased CRI and CQS values, and the higher glowing transition of this double-layer remote phosphor structure, compared to that of the single-layer one which does not include the red phosphor film. The rest of the issue relies upon the objective of the producer, which offers the fitting focus $\text{MgSr}_3\text{Si}_2\text{O}_8:\text{Eu}^{2+}, \text{Mn}^{2+}$ when creating these WLEDs in mass.

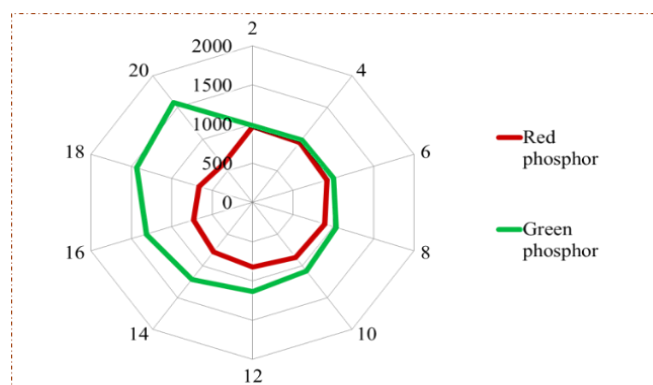


Figure 6. The luminous flux as a function of the concentration of $\text{YF}_3:\text{Er}^{3+}, \text{Yb}^{3+}$ and $\text{MgSr}_3\text{Si}_2\text{O}_8:\text{Eu}^{2+}, \text{Mn}^{2+}$ phosphors

4. CONCLUSION

The paper proposes the impact of phosphor green $\text{YF}_3:\text{Er}^{3+}, \text{Yb}^{3+}$ and phosphor red $\text{MgSr}_3\text{Si}_2\text{O}_8:\text{Eu}^{2+}, \text{Mn}^{2+}$ on CRI, CQS and radiant transition of double layer phosphor structure. In light of the Mie dispersing hypothesis and the Lambert-Beer rule, the examination has demonstrated $\text{MgSr}_3\text{Si}_2\text{O}_8:\text{Eu}^{2+}, \text{Mn}^{2+}$ are reasonable decisions to improve shading quality. In the mean time, $\text{YF}_3:\text{Er}^{3+}, \text{Yb}^{3+}$ is the decision to recuperate the iridescent motion of WLEDs. This isn't valid for WLEDs with low shading temperature however valid for high shading temperature. In this manner, the aftereffects of this examination have accomplished the objective of improving white light shading quality, which is exceptionally troublesome with a remote-phosphor structure. Be that as it may, there is a little drawback that happens with glowing motion. When expanding groupings of $\text{YF}_3:\text{Er}^{3+}, \text{Yb}^{3+}$ or $\text{MgSr}_3\text{Si}_2\text{O}_8:\text{Eu}^{2+}, \text{Mn}^{2+}$ exorbitant, shading quality or glowing motion fundamentally diminished. Subsequently, the decision of a sensible fixation winds up significant, contingent upon the objective of the producer. What's more, the article has given much significant hint to reference in creating better quality WLEDs.

REFERENCES

- [1] Lee H. K., *et al.*, "Color-tunable organic light-emitting diodes with vertically stacked blue, green, and red colors for lighting and display applications," *Optics Express*, vol. 26, no. 14, pp. 18351-18361, July 2018.
- [2] Wanlu Zhang, *et al.*, "Spectral optimization of color temperature tunable white LEDs based on perovskite quantum dots for ultrahigh color rendition," *Optical Materials Express*, vol. 7, no. 9, pp. 3065-3076, September 2017.
- [3] Singh V. K., *et al.*, "Optical studies of erbium and ytterbium doped $\text{Gd}_2\text{Zr}_2\text{O}_7$ phosphor for display and optical communication applications," *Journal of Display Technology*, vol. 12, no. 10, pp. 1224-1228, June.
- [4] Chen L.Y., *et al.*, "Optical model for novel glass-based phosphor-converted white light-emitting diodes," *Journal of Display Technology*, vol. 9, no. 6, pp. 441-446, June 2013.
- [5] Ying S. P., *et al.*, "Curved remote phosphor structure for phosphor-converted white LEDs," *Applied Optics*, vol. 53, no. 29, pp. H160-H164, October 2014.
- [6] Garlick G. F. J., Gibson A. F., "The luminescence of photo-conducting phosphors," *Journal of the Optical Society of America*, vol. 39, no. 11, pp. 935-941, 1949.

- [7] Ying S. P., Shiu A. Y., "Investigation of remote-phosphor white light-emitting diodes with improved scattered photon extraction structure," *Applied Optics*, vol. 54, no. 28, pp. E30-E34, October 2015.
- [8] Kim W. J., *et al.*, "Improved angular color uniformity and hydrothermal reliability of phosphor-converted white light-emitting diodes by using phosphor sedimentation," *Optics Express*, vol. 26, no. 22, pp. 28643-28640, October 2018.
- [9] Schweitzer S., *et al.*, "Improvement of color temperature constancy of phosphor converted leds by adaption of the thermo-optic coefficients of the color conversion materials," *Journal of Display Technology*, vol. 9, no. 6, pp. 413-418, June 2013.
- [10] Yang L., *et al.*, "Preparation of a YAG: Ce phosphor glass by screen-printing technology and its application in LED packaging," *Optics Letters*, vol. 38, no. 13, pp. 2240-2243, July 2013.
- [11] Chen L. Y., *et al.*, "Novel broadband glass phosphors for high CRI WLEDs," *Optics Express*, vol. 22, no. S3, pp. A671-A678, April 2014.
- [12] Jang J. W., *et al.*, "UV-curable silicate phosphor planar films printed on glass substrate for white light-emitting diodes," *Optics Letters*, vol. 40, no. 16, pp. 3723-3726, August 2015.
- [13] Žukauskas A., *et al.*, "Color rendition engineering of phosphor-converted light-emitting diodes," *Optics Express*, vol. 40, no. 16, pp. 26642-26656, November 2013.
- [14] Chiang C. H., *et al.*, "Effects of flux additives on characteristics of $Y_{2.95}Al_5O_{12}:0.05Ce^{3+}$ phosphor: thermal stability and application to WLEDs," *Journal of Display Technology*, vol. 11, no. 5, pp. 466-470, 2015.
- [15] Zhou Z. Z., *et al.*, "White light obtainment via tricolor luminescent centers and energy transfer in $Ca_3ZrSi_2O_9:Eu^{3+}, Bi^{3+}, Tb^{3+}$ phosphors," *Optical Materials Express*, vol. 8, no. 11, pp. 3526-3526, November 2018.
- [16] Kwon O. H., *et al.*, "White luminescence characteristics of red/green silicate phosphor-glass thick film layers printed on glass substrate," *Optical Materials Express*, vol. 6, no. 3, pp. 938-945, March 2016.
- [17] Kuo H. C., *et al.*, "Patterned structure of remote phosphor for phosphor-converted white LEDs," *Optics Express*, vol. 19, no. S4, pp. A936-A936, July 2011.
- [18] Yeh C. T., *et al.*, "Luminescence material characterizations on laser-phosphor lighting techniques," *Optics Express*, vol. 27, no. 5, pp. 7226-7236, February 2019.
- [19] Huang X. Y., *et al.*, "High-brightness and high-color purity red-emitting $Ca_3Lu(AlO)_3(BO_3)_4:Eu^{3+}$ phosphors with internal quantum efficiency close to unity for near-ultraviolet-based white-light-emitting diodes," *Optics Letters*, vol. 43, no. 6, pp. 1307-1310, March 2018.
- [20] Yang T. H., *et al.*, "Stabilizing CCT in pcW-LEDs by self-compensation between excitation efficiency and conversion efficiency of phosphors," *Optics Express*, vol. 25, no. 23, pp. 29287- 29295, November.
- [21] Deng X., *et al.*, "LED power consumption in joint illumination and communication system," *Optics Express*, vol. 25, no. 16, pp. 18990-19003, July 2017.
- [22] Oh J. R., *et al.*, "The realization of a whole palette of colors in a green gap by monochromatic phosphor-converted light-emitting diodes," *Optics Express*, vol. 19, no. 5, pp. 4188-4198, February 2011.
- [23] Wang Q., *et al.*, "Dimmable and cost-effective dc driving technique for flicker mitigation in LED lighting," *Journal of Display Technology*, vol. 10, no. 9, pp. 766-774, September 2014.
- [24] Feng X. F., *et al.*, "LED light with enhanced color saturation and improved white light perception," *Optics Express*, vol. 10, no. 9, pp. 573-585, 2016.
- [25] Choi S. I., "New type of white-light led lighting for illumination and optical wireless communication under obstacles," *Journal of the Optical Society of Korea*, vol. 16, no. 3, pp. 203-209, 2012.